Organic & Biomolecular Chemistry

Accepted Manuscript

This article can be cited before page numbers have been issued, to do this please use: J. Schepper, A. Orthaber and F. Pammer, *Org. Biomol. Chem.*, 2025, DOI: 10.1039/D5OB01979F.

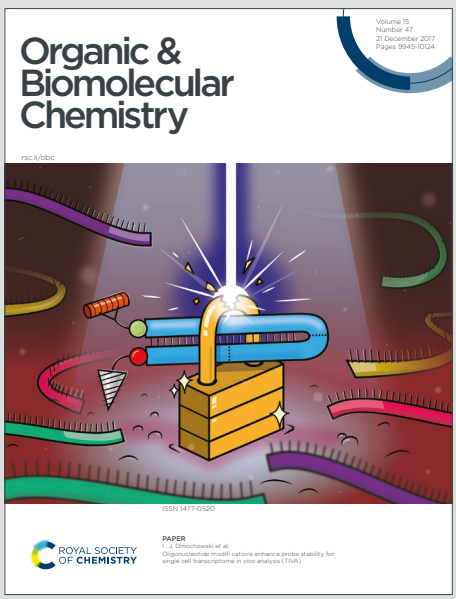

ROYAL SOCIETY OF CHEMISTRY

rsc.li/obc

RESEARCH ARTICLE

View Article Online
DOI: 10.1039/D5OB01979F

Dynamic N→B Coordination and Anion-selective Turn-On Fluorescence in Oxadiazole-functionalized Organoboranes.

Jonas Schepper,[c] Andreas Orthaber,[b] and Frank Pammer*[a]

[a] PD Dr. Frank Pammer
Helmholtz Institute Ulm
Karlsruhe Institute for Technology
Helmholtzstrasse 11, 89081 Ulm, Germany
E-mail: frank.pammer@kit.edu

[b] Prof. Dr. Andreas Orthaber
Department of Chemistry – Ångström laboratories
Uppsala University
BOX 523, 75120 Uppsala, Sweden
E-mail: andreas.orthaber@kemi.uu.se

[c] Dr. Jonas Schepper
Institute of Organic Chemistry II and Advanced Materials
Ulm University
Albert-Einstein-Allee 11, 89081 Ulm, Germany

Supporting information for this article is given via a link at the end of the document.

Abstract: A versatile route for the preparation of chemically and electronically diverse Mes_2BPh-based boranes (Mes = mesityl, 2,4,6-trimethylphenyl) is presented that allows the conversion of tetrazolyl-rings in a common borane precursor (**2H**) into a boranes bearing variously-substituted oxadiazolyl-groups. A series of eight boranes (**4a**–**4h**) was prepared with functional groups on the 5-position of the oxadiazole ranging from electron donating (**4a**: 4-Me-phenyl, **4b**: 4-MeO-phenyl,..) to strongly electron withdrawing (**4d**: 4-O_2N-phenyl, **4e**: 3,5-bis(CF3)-phenyl, **4h**: CF_3) and also including a bifunctionalized example bearing two Mes_2B-moieties (**4g**). A full characterization of the optical, electrochemical and electronic properties, both experimentally and by DFT calculations was carried out.

Our investigation shows the boranes to exhibit dynamic equilibria between ***closed*** intramolecularly N→B-coordinated and ***open*** non-coordinated conformers, as indicated by variable temperature NMR, ^{11}B NMR and anion binding studies with F^- and CN^-. The anion binding studies reveal substantial differences in the fluorescence response of the compounds ranging from differing degrees of quenching to fluorescence shift (**4g**) and enhanced emission **4c** (4-OMe-phenyl). These results show that this synthetic strategy allows to easily create series of compounds with incrementally varied optical properties and Lewis acidities.

Introduction

The exploitation of intramolecular dynamic processes is of increasing interest in current chemical research.[1,2] For instance hemilabile coordination of chelating ligands to transition metals has been recognized as crucial for many catalytic processes,[3] and was exploited in the development of sensing applications.[4]

One of the greatest strengths of organic materials is their large structural variety and the resulting broad range of physical and electronic properties. In this context, the introduction of main group elements into organic scaffolds is being intensively investigated to access new structural motifs and to exploit unusual electronic effects.[5] Introduction of boron[6–14] has attracted particular interest in this regard as it can be incorporated in either the tri-[7,15–17] and tetracoordinate[18–26] form, which give rise to different electronic and chemical properties.

Tricoordinate boron centers in pendant groups[17,27–32] or embedded within π-systems[33–40] lead to a lowering of the Lowest Unoccupied Molecular Orbital (LUMO) and hence increased electron affinity, due to conjugation with their p_z-orbital. Likewise, tricoordinate boranes with tailored Lewis acidity are of great interest as catalysts and chemical sensors.[41–43] Compounds featuring intramolecular N,C^2-chelated tetracoordinate boron (N→B-ladders),[26,44–49] also exhibit increased electron affinity, and have therefore been considered as electron-transporting (n-type) materials.[18–26,50] Recently, N→B-ladders have attracted growing interest, due to promising results in organic light emitting devices,[51] n-channel organic field effect transistors,[52] and organic photovoltaic cells.[23,24,53] The N→B-ladder motive has also been exploited to generate compounds with helical topology.[54–56]

An intriguing feature of ladder boranes is that they can exist in dynamic equilibria between ***closed*** D→B-coordinated (D = N, O, P) and ***open*** non-coordinated conformers (Scheme 1). This behavior is observed, for instance, when the donor atom is part of a heterocycle with low basicity, such as a triazole[57,58] or tetrazole.[59] But also in sterically congested compounds[60] or when strained 4-,[61,62] 7-[63] or 8-membered[64,65] ring systems are formed. Similarly, reduced Lewis acidity at the boron center,[66] and weak Lewis bases such as ethers[67] or carbonyl moieties[68] facilitate dynamic coordination.

Labile D→B- coordination can have a strong influence on the electronic properties of a given π-system (Scheme 1). In the ***closed***, D→B-conformation, the π-system is planarized (Φ ≈ 0°),

RESEARCH ARTICLE

View Article Online
DOI: 10.1039/D5OB01979F

and conjugation along the backbone is more effective, while tetracoordinate boron center acts as an electron-rich inductive donor towards (+I) towards the π^1-ring systems. At the same time, the D→B-interaction exerts an electron withdrawing effect (-I) onto the donor atom (D) in the π^2-ring. In the ***open*** conformation, the empty p_z-orbital on boron exerts a strong electron withdrawing mesomeric effect (-M) on the π-system, while conjugation along the backbone is less efficient due to increased torsion (IΦI >> 0°). Furthermore, in the ***open*** conformation the boron center can act as Lewis acid that can bind nucleophiles (**[Nu→B]**). This latter property of organoboranes has been exploited to develop e.g. chemical sensors for various anions,[69,70] and to develop fluorescent dyes with extreme Stokes' shifts.[67]

A key limitation in the exploration of organoboranes is the limited choice of methods for their preparation. Most commonly used are step-wise metalation.[26,30,34] and electrophilic C-H-borylation.[71,72] Hydroboration of suitable substrates can also yield a broad range of N→B-heterocycles.[24,73–79]

In this report, we demonstrate a versatile synthetic access to compounds capable of labile intramolecular N→B-coordination that builds on our previous work on this topic.

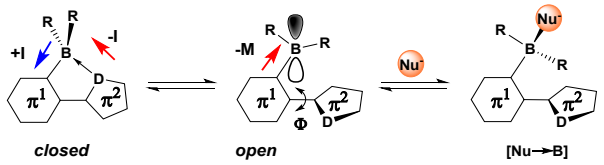

Scheme 1. Conformers of labile coordinated ladder boranes. D: Lewis basic donor atom, N, O, P.

In our group we have developed strategies for the synthesis of N→B-heterocycles by building-up the *N*-heterocyclic component through cycloaddition-reactions. We found that 1,3-dipolar [3+2] azide-alkyne cycloaddition,[57,58] [3+2] azide-nitrile cycloaddition,[59] and cobalt-mediated [2+2+2] cycloaddition between nitriles and alkynes[80] are highly efficient tools for the preparation of electronically and structurally diverse N→B-ladder boranes.

In a recent paper on the synthesis of tetrazole containing organoboranes (Scheme 2A)[59] we reported the preparation of the phenyltetrazole **2H**, which proved to be a versatile starting material for the syntheses described herein: In this paper we have explored the scope of the tetrazole/oxadiazole-conversion for the preparation of a broad range of organoboranes with variable electronic properties (Scheme 2B, Scheme 4).

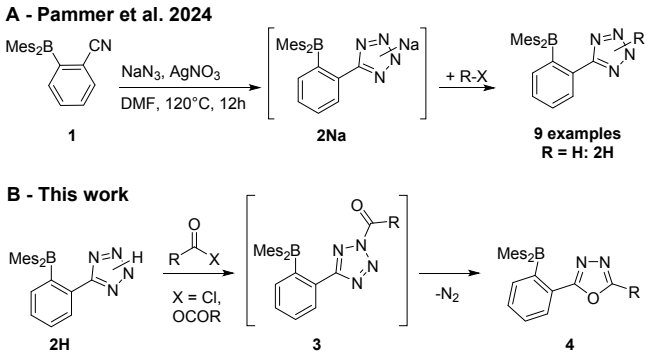

Scheme 2. (A) Preparation of tetrazole-functionalized organoboranes[81] and (B) their conversion into 1,3,4-oxadiazoles.

The tetrazole-ring in **2H** can be acylated to give *N*-acyl-tetrazoles (**3**) which then rearrange into 2,5-disubstituted 1,3,4-oxadiazoles (**4**) under concurrent loss of molecular nitrogen, due to their thermal instability.[81,82] 1,3,4-oxadiazoles have a wide range of applications in pharmaceuticals,[83] and as semiconductors in organic light-emitting diodes (OLEDs).[84,85] Examples of 1,3,4-oxadiazole-based ladder boranes have been reported[86,87] that exhibit thermally activated delayed fluorescence (TADF),[87] and can serve as blue-emitter materials in OLEDs with high electron mobilities.[86]

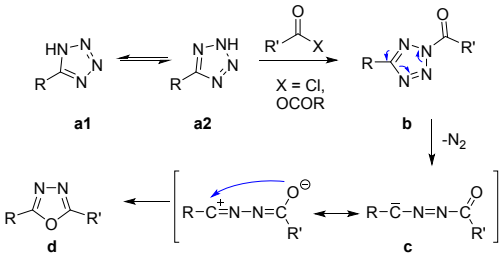

Scheme 3. Mechanism for the conversion of Tetrazoles into 1,3,4-oxadiazoles.[81]

An significant advance over previously reported N→B-ladders is the fully conjugation across the heterocycle in the systems reported herein (Chart 1A, 'type 4'). In triazole-[57,58] (Chart 1B, 'type 5') and tetrazole-[59] (C, 'type 6) containing N→B-ladders substituents could only be introduced on a saturated, conjugation breaking ring-nitrogen (N—). Unsaturated peripheral substituents therefore invariably experience only limited (cross-) conjugation the π-system. In case of tetrazoles (C), the synthesis only allowed the introduction of alkyl-substituents on the ring-nitrogen, which preempts extension of the conjugated system. Due to a lack of boranes with directly comparable π-systems, the experimental data only weakly reflect the improved conjugation in type 4 vs. type 5/6, as we will discussed further on.

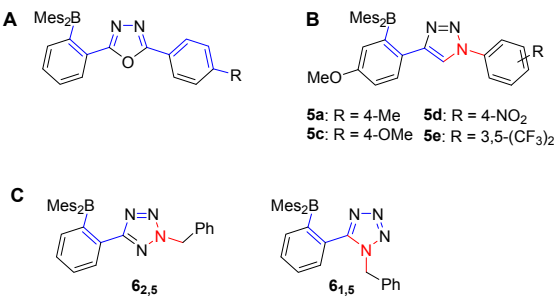

Chart 1. Conjugation across the heterocycle in different N→B-ladder boranes. —: Maximum conjugated pathway starting at boron. **A**: Oxadiazoles in this work, **B**: Triazoles adopted from ref. [57] (see also ref. [58]). **C**: Tetrazoles adopted from ref. 69. N—: Conjugation breaking atom/bonds. R: functional groups.

RESEARCH ARTICLE

View Article Online
DOI: 10.1039/D5OB01979F

Results and Discussion

Synthesis and structure

The oxadiazole synthesis was tested and optimized by acylating tetrazole **2H**[59] with *p*-toluoyl chloride (→**3a**) at ambient temperature and subsequent conversion into the 1,3,4-oxadiazole **4a** (Table 1) at different temperatures. Upon addition of *p*-toluoyl chloride to a suspension of **2H** in toluene, the reaction mixture immediately turns intensely yellow in color attributed to the formation of acyltetrazole **3a**. Upon heating foaming and gas evolution can be observed as deazotation sets in and the yellow coloring steadily fades. When the deazotation reaction was carried out at 110 °C, the corresponding oxadiazole **4a** could be isolated in a yield of 35% after purification by column chromatography (Table 1). Lower (90 °C) and higher (130 °C) reaction temperatures gave significantly lower yields of 15% and 13%, respectively (see Table 8). To increase the yield, different bases (NEt_3 and K_2CO_3) were added to trap the liberated HCl. The use of NEt_3 did not result in a substantial increase in yield, but addition of K_2CO_3 allowed near quantitative isolation (95%) of **4a**. Comparison of NMR experiments with and without addition of K_2CO_3 (see Figure S1A in the ESI) showed that mesitylene (Mes-H) is formed after heating to 110 °C when no base is present, likely due to protolysis of the B-Mes bonds in **2H**, **3** or **4** by HCl (see Figure 1A). In contrast, Mes-H-formation cannot be observed when K_2CO_3 is added, since the base effectively captures the acid (see Figure S1A in the ESI). The protolysis would initially produce boryl-chloride **7** (Figure 1A) which can react further to more the chemically robust borinic acids (**8**) through reaction with trace moisture or OH^- from the glass of the reaction vessel or during workup. This was confirmed in the synthesis of compound **4b**, with the isolation of **8b** (see Figure 1) when no basic additive was used.

Table 1. Optimization of the oxadiazole synthesis based on the reaction of the tetrazole **2H** with p-toluoyl chloride.[a]

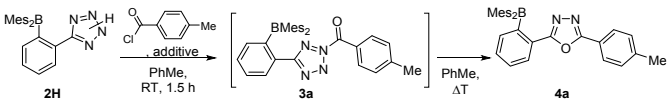

Temperature [°C]	Additive (7 equiv.)	Isolated Yield [%]
90	-	15
110	-	35
130	-	13
110	NEt_3	39[b]
110	K_2CO_3	95

[a] Solvent: toluene, acylation reaction carried out at room temperature. [b] Approximate yield, contained an unidentified impurity.

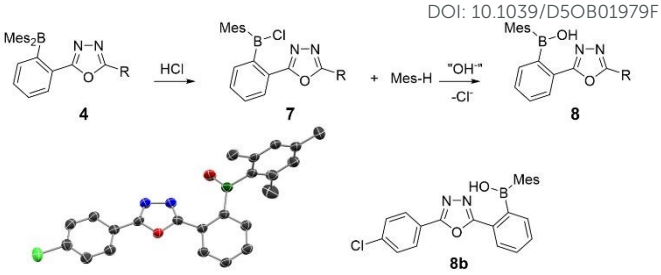

Figure 1. Top: Example for the formation of borinic acids **8.** Bottom: crystal structure of borinic acid **8b**, which was crystallized during the workup of compound **4b**; Ellipsoids shown with 50% probability; Hydrogen atoms have been omitted for clarity.

With the reaction conditions optimized as described above, seven other 5-aryl-substituted 1,3,4-oxadiazoles could be synthesized using commercially available acid chlorides (see Scheme 61). The oxadiazoles **4a** to **4f** were isolated in very good yields of 84-99%. The diborylated compound **4g**, which is accessible by using terephthalic acid dichloride as acylating agent, could be isolated in only 36% yield. Both electron rich (**4a**, **4c**) and electron poor (**4d**, **4e**) aryl groups work equally well, with the exception of the 4-dimethylamino-derivative (**4i**), which could not be generated.

A 5-CF_3-substituted oxadiazole (**5h**) was synthesized by acylation with trifluoroacetic anhydride.[88] The corresponding acyltetrazole **3h** is significantly less thermally stable with deazotation occuring at room temperature immediately after its formation. After purification by column chromatography, the CF_3-functionalized oxadiazole **4h** could be isolated in 23% yield.

This is immediately apparent from the ^{11}B NMR spectra of compounds **4a** to **4f** (Figure 3A/B): The chemical shift of the ^{11}B signals correlates linearly (R^2 = 0.947) with the Hammet substituent parameter σ of the respective substituents on the phenyl ring, which can serve as a measure for electron-withdrawing or electron-donating effects of the respective substituent.[57,89] **4g** and **4h** had been omitted from Figure 3, since σ values cannot be given for these compounds. We have included DFT data for **4i** (Scheme 4), however, which could not be synthesized but was included in the computation survey.

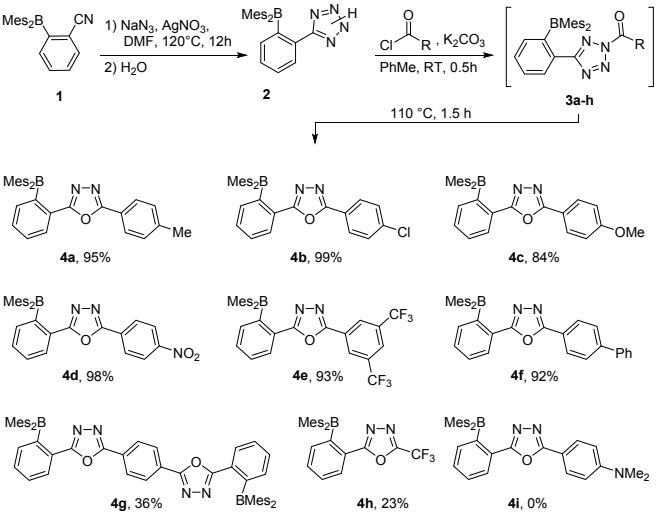

RESEARCH ARTICLE

View Article Online
DOI: 10.1039/D5OB01979F

Scheme 4. Synthesis of the borylated 1,3,4-oxadiazoles **4a** to **4h** starting from tetrazole **1**. **4i** did not form, but is included in the computational survey.

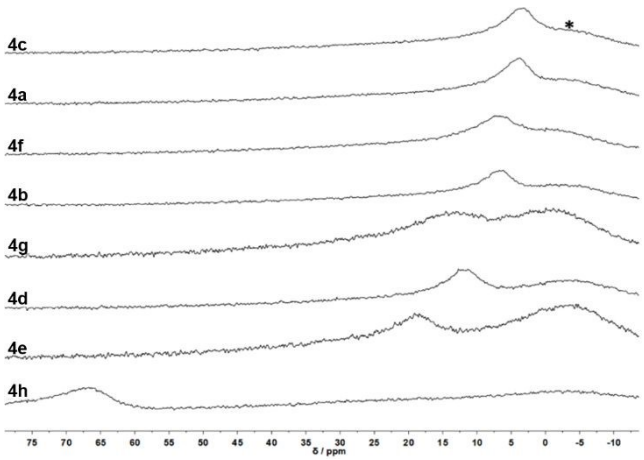

Figure 2. ^{11}B NMR spectra of the synthesized oxadiazoles. Recorded in either THF-d_8 (**4a** – **4f**, **4h**) or DCM (**4g**); * glass background signal.

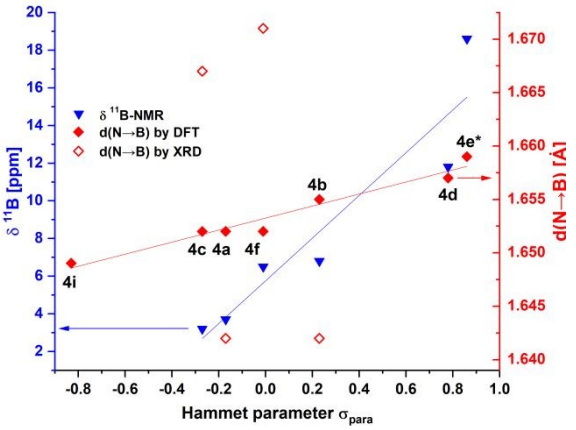

Figure 3. Correlation between Hammet parameters and experimental ^{11}B NMR chemical shifts (▼) and N→B-bond length derived by DFT (◆) and experimental X-ray diffraction (◇). *__4e__: σ = 2*$\sigma_m(CF_3)$ = 0.86.

The more electron-rich oxadiazoles exhibit the most upfield ^{11}B chemical shifts with signals at 3.7 ppm (**4a**) and 3.2 ppm (**4c**), which is within the range of four-coordinate boron centers of the form N→BAr_3. Oxadiazoles with more neutral substituents exhibit slightly downfield ^{11}B chemical shifts of 6.8 ppm (**4b**) and 6.5 ppm (**4f**), while for compounds with strongly electron-withdrawing groups **4d** (-NO_2) and **4e** (*m*-CF_3) clearly downfield-shifted ^{11}B signals are observed at 11.8 ppm (**4d**) and 18.6 ppm (**4e**), respectively. The latter values fall into the range of N-alkylated phenyltetrazoles[59] for which labile N→B-coordination was established. Oxadiazole **4g** is only marginally soluble in THF, but shows an ^{11}B chemical shift of 13.1 ppm in DCM, in the same range as **4b** and **4e**. Compound **4h** exhibits the most downfield ^{11}B chemical shift among the synthesized oxadiazoles of 67.1 ppm. A value in this range suggests a purely three-coordinate boron center like Mes_3B(79.0[90] ppm) or BPh_3 (60.2[91] ppm).[70] N→B-interactions do therefore not occur in **4h**.

Single crystals suitable for X-ray diffraction analysis were obtained of oxadiazoles **4a**, **4b**, **4c**, and **4f**. The crystals were grown either by diffusion of n-pentane into THF solutions or by slow evaporation of THF solutions. The structures show all four compounds to adopt ***closed*** N→B-coordinated geometries in the solid state (see Figure 4). As a result, the π systems are almost planarized with torsion angles between the oxadiazole and the $PhBMes_2$ unit of 4.5° (**4a**), 5.1° (**4b**), 3.8° (**4c**) and 5.6° (**4f**). Curiously, unlike the ^{11}B chemical shift, the experimental bond lengths do not correlate with the substituents on the phenyl ring. With respect to the N→B bond lengths **4a** (1.642(3) Å) and **4b** (1.642(2) Å) form comparatively short bonds, with those in **4c** (1.667(5) Å) and **4f** (1.671(2) Å) are significantly longer. Bond lengths in **4a** and **4b** are comparable to those in *N*-benzyl-tetrazole-derivative $\mathbf{6}_{1,5}$ (1.643(8) Å, Chart 1),[59] while those in **4c** and **4f** are far longer than N→B-bonds in the structurally closely related triazole-based boranes **5a** (1.632(2) Å), **5d** (1.638(4) Å) and **5i** (1.630(3) Å).[57] This broad variation stands in contrast to the bond lengths in computed structures, which correlate very well with the Hammet parameter σ (see "◆" in Figure 3, R^2 = 0.957). At first glance this correlation in itself might just be a reflection of a systemic error. However, for the structurally closely related type 5 boranes[57] linear correlations (see **Table 2**, see also Figure S58 in the ESI) were found for both computed and experimental N→B-bond lengths, even though the calculations systematically over-estimated the N-B-distance. We therefore tentatively attribute the large deviations to packing effects in the solid state.

Table 2. Experimental and computed properties of synthesized boranes and reference compounds.

#	Com-pound	R on Ph-ring	σ[a]	^{11}B-NMR[b] [ppm]	N→B bond lengths in Oxadiazoles XRD[c] [Å]	N→B bond lengths in Oxadiazoles DFT[d,e] [Å]	N→B bond lengths in 1,2,3-Triazoles[r] XRD[c] [Å]	N→B bond lengths in 1,2,3-Triazoles[r] DFT[d,e] [Å]	$\Delta G_{open/closed}$[e,f] Neutral[f] [kJ/mol]	$\Delta G_{open/closed}$[e,f] Anions[f] [kJ/mol]	FIA[e,g] [kJ/mol] vs. *open* [kJ/mol]	FIA[e,g] [kJ/mol] vs. *closed* [kJ/mol]
1	**4a**	4-Me	-0.17	3.7	1.642(3)	1.652	1.632(2)	1.668	+4.9	-8.3	307.4	302.5

View Article Online
DOI: 10.1039/D5OB01979F

2	**4b**	4-Cl	0.23	6.8	1.642(2)	1.655		1.671	-4.7	-3.4	317.2	321.8
3	**4c**	4-OMe	-0.27	3.2	1.667(5)	1.652		1.668	+1.8	-8.2	306.9	305.1
4	**4d**	4-NO_2	0.78	11.8	-	1.657	1.638(4)	1.678	+4.4	45.3	363.9	359.5
5	**4e**	3,5-$(CF_3)_2$	0.86	18.6	-	1.659		1.678	-18.3	28.4	326.8	345.1
6	**4f**	4-Ph	-0.01	6.5	**closed**	**1.652**			**-7.0**	**-7.7**	313.0	314.3
7	**4g**	n.a.[h]	n.a.	13.1[i]	-	1.656			-5.3[j]/-11.6[k]	-69.86[l] /+101.3[m]	348.0[n]	353.3[o]
8	**4h**	CF_3[h]	n.a.	67.1	-	1.667			-12.5	-5.3	318.8	331.2
9	**4i**[p]	4-NMe_2	-0.83	--		1.649	1.630(3)	1.676	+7.4	-13.7	301.5	294.1
10	**Mes_3B**[p]			79.0[90]								287.7
11	**Mes_2BPh**[p]			79.5[90]								301.8
12	**$MesBPh_2$**[p]			n.a.								309.4
13	**BPh_3**[p]			60.2[91]								331.8
14	**$B(C_6F_5)_3$**[p]											471.4[q]

[a] *para*-Hammett parameter, see ref. [89] **4e**: $\sigma = 2*\sigma_m(CF_3) = 0.86$. [b] Experimental ^{11}B NMR shifts measured in THF-d_8. [c] Experimental N→B-bond lengths derived from crystal structures. [d] N→B-bond lengths in simulated structures, [e] Level of theory M06-2X/TZVP. [f] ΔG of *open* vs. *closed* conformations in the neutral boranes and radical anions respectively; [g] Fluoride ion affinities vs. both ***open*** and ***closed*** conformers. The lower FIA corresponds to the more stable conformer. See text for details. [h] **4g**: Does not apply. **4h**: 5-CF_3-oxadiazolyl. See **Scheme 4** for structures. [i] Recorded in CD_2Cl_2. [j] [***open***/***open***] vs. [***closed***/***closed***]. [k] [***open***/***open***] vs. [***closed***/***open***]. [l] **4g**$^{-1}$ [***open***/***open***] vs. [***closed***/***closed***. [m] **4g**$^{-2}$ singlet, [***open***/***open***] vs. [***closed***/***closed***]. [n] FIA of **4g**: [(F→B)/***closed***] vs. [***open***/***open***], [o] FIA of **4g**: [(F→B)/***closed***] vs. [***closed***/***closed***]. [p] Not synthesized. Only included in the DFT-survey. [q] Ref. [43] report 444 kJ/mol for this compound using BP86/SV(P). [r] Data for triazoles adopted from ref [57].

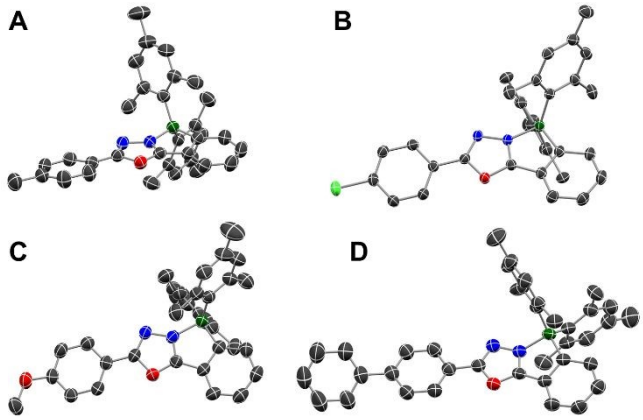

Figure 4. Crystal structures of the oxadiazoles **4a** (A), **4b** (B), **4c** (C) and **4f** (D); Ellipsoids shown with 50% probability; Hydrogen atoms have not been shown for clarity.

The rotational barrier around the C_{Mes}-B bond could also be determined for compound **4a** using variable temperature NMR spectroscopy (see Figure S17 in the ESI), whereby a coalescence temperature for the aromatic mesityl signal of 242 K was observed, corresponding to a $\Delta G_C = 47.7 \pm 0.3$ kJ/mol, which is in a similar range as for tetrazole-based N→B-ladders.[59]

Electrochemical Properties

The electrochemical properties of the oxadiazoles, were checked by cyclic voltammetry (CV) and square-wave voltammetry (SWV) (see Section 2.5 the in ESI). CV allowed to classify the ir-/reversibility of electrochemical reduction processes while the first peak potentials observed in SWV served to calculate the energies of the lowest unoccupied molecular orbitals (LUMO) (E_p^{red} see Figures S40 and S47 in the ESI). The acceptor substituted compounds **4d**, **4e**, **4g** and **4h** exhibit higher electron affinities than the parent borane **1** (E_p^{red} = -2.22 V vs. FcH/FcH$^+$, E_{LUMO} = -2.88 eV), with **4d** showing the highest electron affinity at -1.38 V (E_{LUMO} = -3.72 eV). Boranes with electron-rich (**4a** and **4c**) or neutral (**4b** and **4f**) substituents provide electron affinities that are lower than or comparable to borane **1**, respectively.

All oxadiazoles show only irreversible reductions (see Figure S39), with the exception of **4e** and **4g**, which show quasi-reversible reductions at -1.99 V and -1.84 V (vs. FcH/FcH$^+$), respectively. Only one reduction could be observed for compounds **4a**, **4c**, **4g** and **4h**. These reduction events are presumed to involve the empty p-orbital on boron.[57,58] For the other oxadiazoles, between two (**4b**, **4e**, **4f**) and four reductions (**4d**) were detected. The two-fold reduction of **4b** may be caused by electrochemical dechlorination[92] and subsequent reduction of the defunctionalized borane, whereas two-fold reduction of **4e** and **4f** is deemed to be a combination of reduction at the boron center and injection of an electron into the 5-aryl-oxadiazole π-system. The first reduction of **4d** (-1.38 V vs. FcH/FcH$^+$) is likely associated with a redox process centered on the nitro group since the potential is in the typical range of nitro-arenes.[93] The origin of the other processes is unclear, but may involve reduction at the boron center, injection of electrons into the 5-aryl-oxadiazole π-system or reductive degradation of the nitro-group.

Optical and electronic properties

To characterize the optical properties of the boranes, absorption and fluorescence spectra were recorded in DCM solution (see Figure 5A/B). All boranes exhibit absorption maxima between 292 and 325 nm accompanied by a shoulder band towards longer wavelength. The underlying longest wave-length absorption band (λ_{max}) that gives rise to the shoulder has been derived for all compounds by Gaussian deconvolution of the experimental spectra (see Table 3 and Figures S3-S10 in the ESI). Its intensity relative to the main band varies significantly. We were able to conclude that λ_{max} is associated with electronic transitions involving the empty p_z-orbital on boron in ***open***, non-N→B-coordinated conformers, as it is suppressed in the presence of strong nucleophiles (see below). An exception to this is **4d**

RESEARCH ARTICLE

View Article Online
DOI: 10.1039/D5OB01979F

wherein the strongly accepting NO_2-group rather than the $BMes_2$-group dominates the optical properties. **4h** shows the lowest energy λ_{max} (385 nm / 3.25 V) followed by **4g** (369 nm / 3.36 eV) and **4d** (362 nm / 3.43 eV), while the remaining boranes show values within ±0.05 eV of the parent borane **1** (346 nm, 3.58 eV), with the notable exception of the more electron rich **4a** (338 nm / 3.67 nm).

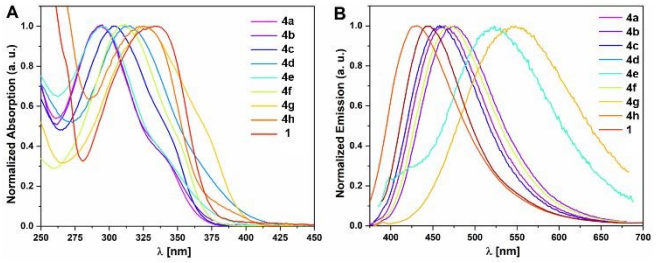

Figure 5. UV-vis Absorption (A) and Fluorescence (B) spectra of the oxadiazoles. Recorded in DCM.

With the exception of the NO_2-functionalized oxadiazole **4d**, all oxadiazoles synthesized here exhibit fluorescence with emission maxima between 430 nm (**4h**) and 544 nm (**4g**). Compounds **4a** through **4g** show quantum yields of 33-35% with large Stokes shifts of between 6480 cm^{-1} (**4a**) and 6542 cm^{-1} (**4e**). **4h** constitutes an exception with a Φ of 4% and a much smaller Stokes shift of 2922 cm^{-1}. The latter may be readily explained by the smaller molecular size of **4h** which consequently allow for less charge redistribution upon excitation.

Anion Binding

Tricoordinate boron centers can bind various nucleophiles such as fluoride or cyanide anions.[57,59,70,80] To investigate the influence of anion binding on the optical properties in more detail, absorption and emission spectra were recorded after addition of an excess of tetrabutylammonium fluoride (TBAF) and tetrabutylammonium cyanide (TBACN) as fluoride and cyanide sources, respectively (see Figure 6). With the exception of oxadiazole **4d**, all oxadiazoles in the survey show a blue shift in the absorption that corresponds to a suppression of the λ_{max} band. We attribute this to binding of the anions to the boron center, because the empty p_z-orbital contributes strongly to the LUMO of all ***open***-conformers except **4d-*open*** (see Figure S51 to S53 in the ESI). The LUMO is bound to participate in the lowest energy excitation. Consequently, binding of nucleophiles renders this electronic transition inaccessible. This is corroborated by experimental data on **4d**: Here, the main absorption band is being suppressed in the presence of an anions, but the onset remains unaffected. Orbital plots show the p_z-orbital to contribute only to the LUMO+1 of **4d-*open***. Binding of nucleophiles is therefore expected to affect a higher energy transition, not the λ_{max}-band.
The nature of the anion does not seem to have a significant influence on the absorption properties of the oxadiazoles, as can be deduced from the very similar spectra of the fluoride- and cyanide-bound oxadiazoles.

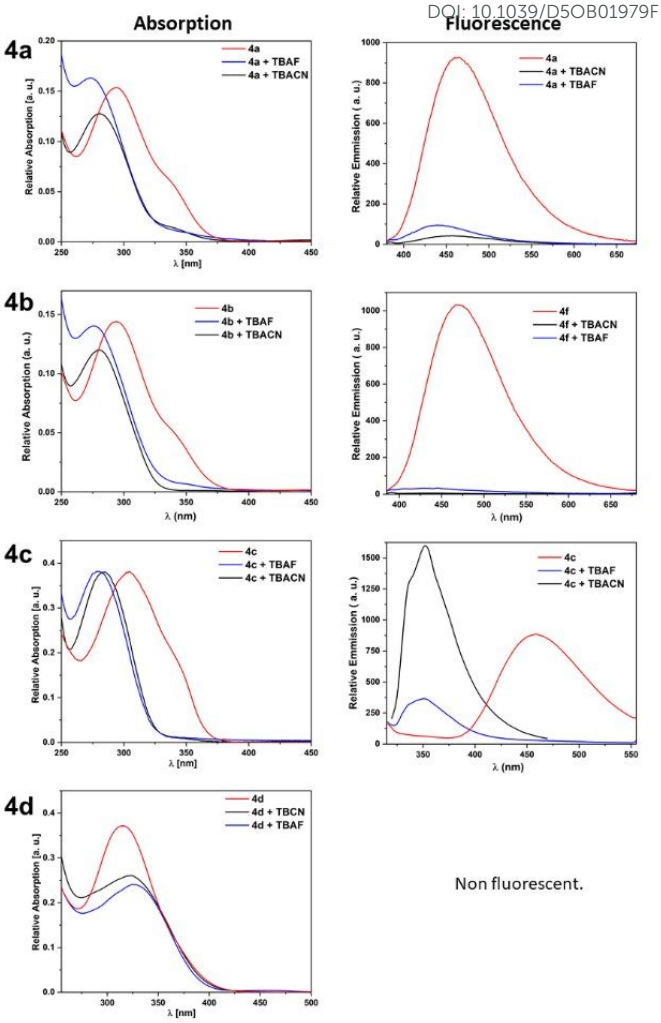

Figure 6.1. Normalized absorption and emission spectra of the synthesized oxadiazoles without and with the addition of an excess of TBAF or TBACN. Recorded in DCM.

RESEARCH ARTICLE

View Article Online
DOI: 10.1039/D5OB01979F

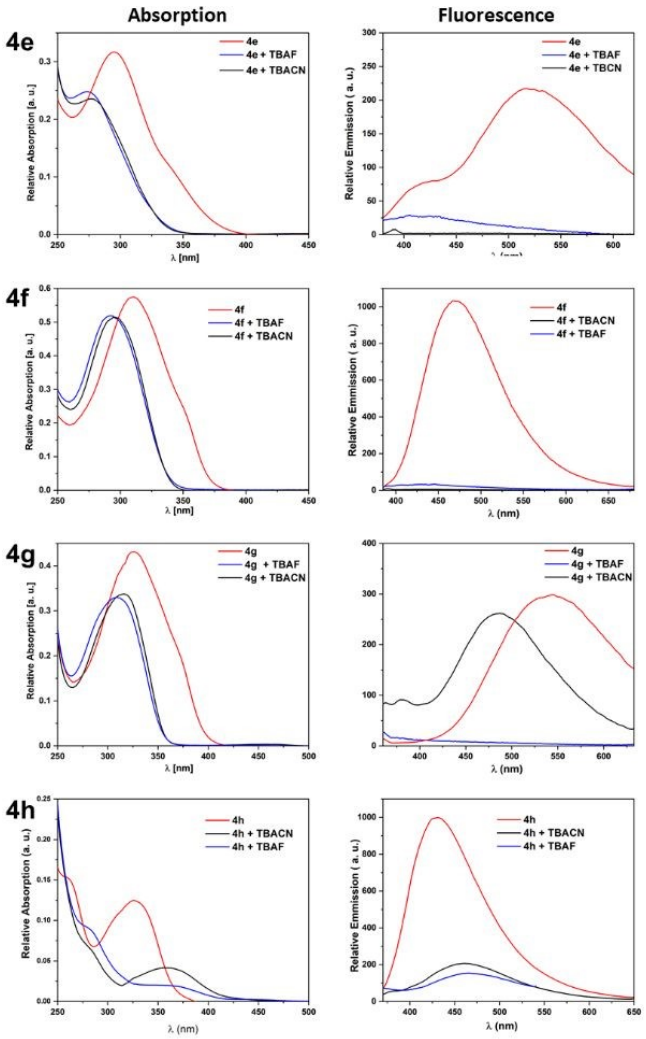

Figure 6.2 Normalized absorption and emission spectra of the synthesized oxadiazoles without and with the addition of an excess of TBAF or TBACN. Recorded in DCM.

The situation is somewhat different with regard to the fluorescence behavior. For most compounds (**4a**, **4b**, **4e**, **4f** and **4h**), the fluorescence intensity is partially (**4a**, **4e**, **4h**) or fully suppressed regardless of the involved nucleophile (see Figure 6). In contrast, in the case of the OMe-substituted oxadiazole **4c**, the addition TBAF and TBACN leads to a blue shift of the emission from 459 nm to 351 nm (see Figure 6). However, while TBAF effects a partial suppression of the emission, addition of TBACN leads to a significant increase in emission. The most interesting behavior has been observed for **4g**: Here, complete fluorescence quenching is observed upon addition of TBAF, whereas a blue shift of the emission from 544 nm to 486 nm occurs upon addition of TBACN (see Figure 6F). This means that the oxadiazoles **4c** and **4g** are generally suitable to serve as fluorescence-based anion sensors. For **4c** the fluorescence spectra of the pristine borane and of the F^{-1}-saturated species (**4c-F**) form an isosbestic point at 395 nm, while the emission intensity after addition of TBACN is more intense at this wavelength. Consequently, selective detection at this wavelength allows discrimination between CN^- and F^-. A similar approach is possible for **4g**. Below 504 nm fluorescence of **4g-CN** is more intense than that of **4g**, while F^--addition quenches the emission altogether. At ca. 408 nm residual fluorescence of **4g** and **4g-F** reach barely above the background, while emission from **4g-CN** significantly more intense.

Table 3. Summary of the optoelectronic properties of oxadiazoles **4a** -**4h**.

Com-pound.	E_p^{red}[a] [V]	LUMO[c] [eV]	λ_{max}[d] [nm]	λ_{onset} [nm]	E_g^{opt}[e] [eV]	λ_{em} [nm]	Stokes Shift[f] [cm^{-1}]	Φ[g] [%]
CN	-2.22r	-2.88	346	385	3.22	446	6480	
4a	-2.41i	-2.70	338	367	3.38	463	7988	34
4b	-2.25i -2.36i	-2.85	342	372	3.33	475	8187	33
4c	-2.43i	-2.67	345	366	3.39	459	7199	34
4d	-1.38qr -1.63qr -1.90i -2.37i	-3.72	362	380	3.26	-	-	-
4e	-1.96r -2.56i	-3.14	348	378	3.28	521	9542	n.d.
4f	-2.24i -2.81i	-2.86	349	371	3.34	470	7377	35
4g	-1.85r	-3.25	369	397	3.12	544	8718	n.d.
4h	-2.09i	-3.01	382	408	3.04	430	2922	4
5a[i]	-2.64r	-2.46	330	360	3.44	380	3990	1
5c[i]	-2.63r	-2.47	350	379	3.27	384	2530	2
5d[i]	-1.52r	-3.58	360	417	2.97	-	-	n.f.
5e[i]	-2.19r	-2.91	330	386	3.21	-	-	n.d.
6a[j]	-2.58		314	352	3.52	444	9325	93
6b[j]	-2.66		337	353	3.51	n.d.	-	-

[a] Peak-Potential determined via Square-Wave-Voltammetry in THF with 0.1 M [N*n*Bu$_4$][PF$_6$], scan-speed 0.1 V/s; [b] Determined via Cyclic Voltammetry, scan-speed 0.2 V/s [c] Relative to the LUMO-Energy of Ferrocene (−5.1 eV)[94]; [d] Derived by deconvolution. See section 2.3 of the ESI; [e] Derived from λ_{onset}; [f] Derived from λ_{max} und λ_{em}; [g] Measured with an Ulbricht-integrating sphere. [h] Data adopted from reference 68. [h] Data adopted from reference. [i] Data adopted from reference [59].

Comparison vs. triazole- and tetrazole-N→B-systems: Previously published triazole-based borane either included two Mes_2B-functionalities,[58] or bore an electron donating methoxy-substituent on the borylated ring (**5a**, **5c-e**, 'type 5',Chart 1B),[57] while tetrazoles were invariable equipped with non-conjugated substituents on the heterocycle. (**6$_{1,3}$/6$_{1,5}$** 'type 6', Chart 1C). Directly comparisons therefore need to be approached with caution. Type-**4**-systems show higher electron affinities (**E_p^{red}**) than type 5 and type 6 systems. However, for type 5s this may be owed to the OMe-Group which is not directly conjugated to the Mes_2B-group, but nevertheless donates electrons to the π-system as a whole. For *N*-alkyl-substituted type 6-boranes, no equivalent exists in the current dataset. The optical gaps of type 4 and type

View Article Online
DOI: 10.1039/D5OB01979F

5 boranes are comparable, and thus do not reflect a more effective conjugation. Again, this may be owed to a donor-acceptor-interaction between the OMe-group and the electron poor triazole ring. Type 4 exhibit larger Stokes shifts ($\mathbf{4_a}$ vs. $\mathbf{5_a}$ and $\mathbf{4_c}$ vs. $\mathbf{5_c}$), which points towards more pronounced intramolecular charge redistribution or conformational changes but is no .

Computational study

Structure and conformation: In addition to the experimental studies, DFT simulations of the oxadiazoles were carried out. The geometry-optimized molecular structures show N→B bond lengths between 1.652 Å (**4c**) and 1.667 Å (**4h**), which are longer than the simulated bond lengths of the phenylpyridines (1.646 Å - 1.649 Å.[80]). Oxadiazoles with electron-donating substituents show shorter N→B bond lengths (**4a** :1.652 Å, **4c**: 1.652 Å, **4f**: 1.652 Å) than compounds with electron-withdrawing substituents (**4d**: 1.657 Å, **4e**: 1.659 Å, **4h:** 1.667 Å). These results are consistent with the experimental ^{11}B chemical shifts, which suggest a higher electron density at the boron center for the more electron-rich substituents.

Furthermore, we compared the energies of ***open*** and ***closed*** N→B-coordinated conformers. The correlation of the Gibbs free energies of the indicates that the substituents on the oxadiazole regulate whether a ***closed*** N→B-coordination is favored over an ***open*** conformation (see Table 2). Boranes bearing strong acceptors (**4d**: $\Delta G_{o/c}$ = -11.8 kJ/mol, **4e**: -18.3 kJ/mol, **4h**: -12.5 kJ/mol) favor the ***open*** conformations. This may be attributed to the lower basicity of the oxadiazole-nitrogen due the electron withdrawing functional groups. The reduced energetic gain from the N→B coordination, cannot overcome the increased steric crowding around the tetrahedral boron center. Donor-substituted oxadiazoles (**4a**: $\Delta G_{o/c}$ = +4.9 kJ/mol, **4c**: +1.8 kJ/mol, **4i**: +7.4 kJ/mol) slightly favor the ***closed*** conformation. The effect is not large, however, and lies within a range of thermally accessible at ambient temperature. ***Open*** and ***closed*** conformers of all compounds can therefore exist in dynamic equilibrium.

The conformers of compounds introduced herein cover slightly broader energetic range of about 25 kJ/mol (+7 kJ/mol to -18 kJ/mol) – comparable to similarly labile N→B coordinating tetrazolyl-[59] (+2 to -16 kJ/mol) and triazolyl-functionalized[57,58] (0 to -20 kJ/mol) functionalized boranes. This may be owed to the more direct conjugation to functional group, but could equally be caused by subtle differences in the coordination chemistry of oxadiazoles.

Radical anions: To link the molecular structures with the electrochemical properties, we also modelled radical anions of ***open*** and ***closed*** conformers (Table 2). This study showed the almost exactly inverse correlation as the neutral boranes: In the reduced state, systems with strong acceptors (**4d**$^{-1}$, **4e**$^{-1}$) strongly favor the ***closed*** conformation. This can be explained by a comparison of lowest unoccupied orbitals (LUMO) of the neutral boranes (see Figures S48-S51 in the ESI) and the spin density plots (SDP) of the radical anions (see Figures S53 and S54 in the ESI): Both LUMO and SDP of ***open*** conformers generally show strong contributions from the empty p_z-orbital on boron, whereas ***closed*** conformers exhibit extended delocalization throughout the planarized π-system. The electron rich or neutral systems (**4a**, **4b** **4c**, **4f**, **4i**) slightly favor **open**$^{-1}$ (-3.4 to -13.7 kJ/mol) in rough correlation with the donor strength of the functional group. Thereby, interaction with the electron rich donor-substituted π-system is avoided. In contrast, the presence of strong acceptors (**4d**, +45.3 kJ/mol; **4e,** +28.4 kJ/mol) strongly favors ***closed*** conformers wherein the interaction between the functional group and π-system seems maximized.

The situation is somewhat special in the diborylated **4g**. The neutral borane slightly favors a ***closed/open*** (-5.3 kJ/mol) or ***open/open*** (-11.6 kJ/mol) conformation over a ***closed/closed*** arrangement. This trend is amplified in the radical anion **4g**$^{-1}$ (-69.9 kJ/mol) which in the ***open/open***$^{-1}$ conformation benefits from stabilization both by one empty p_z orbital and delocalization and across both oxadiazole rings in the wider π-system. In contrast, for the singlet dianion **4g**$^{-2}$ the ***open/open***$^{-2}$-conformation is strongly disfavored (+101.3 kJ/mol). While the HOMOs of both the ***open/open***$^{-2}$ and the ***closed/closed***$^{-2}$–conformers involve delocalization across the whole π-system (see Figure S52 in the ESI), the ***closed/closed***$^{-2}$ conform shows an evidently more effective conjugation across the planarized ringsystem

Compared to other N→B-compounds, the range of energetic de-/stabilization of the ***closed*** conformers is broader for the oxadiazoles investigated herein compared to tetrazoles (**2**, Scheme 2[59]), but much weaker than in pyridine-based compounds.[80]

Origin of optical properties: To elucidate the origin of the optical properties of the boranes, time-dependent DFT calculations (TDDFT) were performed at the M06-2X/Def2-TZVP level with the PCM solvent model and dichloromethane as solvent. The obtained electronic transition allowed the generation of UV-Vis-absorption spectra that are in qualitative agreement with the experimental data (see Figures S55 and S56 and Tables S6 and S7 in the ESI). According to the calculations the lowest energy transitions in ***open*** conformers generally involve a charge transfer from an electron rich π-orbital (HOMO or HOMO-1) towards the empty p_z-orbital on boron, which generally dominates the LUMO except when the very strongly electron withdrawing –NO_2-group is present (**4d**). In that case, the p_z-contributes to LUMO+1.

The HOMO and HOMO-1 tend to be delocalized across the mesityl-rings attached to boron, unless strong donors like –NMe_2 (**4i**), -OMe (**4c**) or -Ph (**4f**) are present. Presumably, the very electron poor oxadiazole ring also lowers the frontier orbital energies of the π-system across the conjugated neighboring phenyl rings and thereby leaves the more electron rich mesityl-rings to dominate the highest occupied orbitals. This effect is partially compensated by donor-acceptor-conjugation in **4i**, **4c** and **4f**. Because of the very limited spatial overlap the intensity of this transition – as indicated by the oscillator strength f – is expected to be very low (f = 0.036 (**4i**) to 0.125 (**4d**)).

The lowest energy transitions in ***closed*** conformers always involves a charge transfer from the mesityl-groups towards π*-orbitals delocalized across the Ph-oxadiazole-Ph-π-system Apparently, the stronger +I-effect of the tetrahedral boron center renders the Mes-groups much more electron rich. Only the strong

View Article Online
DOI: 10.1039/D5OB01979F

donor –NMe_2 leads to marginal conjugation across the Ph-oxadiazole-Ph-π-system in its HOMO.
Lowest energy transitions in most ***open*** conformers are 0.1 to 0.24 eV lower in energy than in ***closed*** ones, but electronic coupling seems more efficient in ***closed*** conformations with *f* being between 2x (**4e**) and 34x (**4i**) higher than in the corresponding ***open*** conformers. This corroborates the assumption that the longest-wavelength shoulder band in the absorption spectra originates from the ***open*** conformers.

Fluoride Ion Affinity (FIA): To further assess the Lewis-acidity of the individual boranes, fluoride-ion affinities (FIA) have been calculated at the M06-2X/TZVP level in the gas phase according to the following model reaction (see Table 2 for results).

$$[\text{Borane}] + F^{-1} \rightarrow [\text{Borane-F}]^{-1} \quad (1)$$

Included in the survey were the oxadiazole-containing boranes **4a** through **4i**, along with Mes_3B, Mes_2BPh, $MesBPh_2$, BPh_3, and $B(C_6F_5)_3$ to provide a frame of reference. For boranes **4a** through **4i** FIAs – expressed as -ΔG of the model reaction in kJ/mol – have been computed for both ***open*** and ***closed*** forms. For the subsequent discussion the lowest FIA of the two is considered the most relevant, because it represents the transition between the most stable neutral conformer and the $[\text{Borane-F}]^{-1}$-complex.
The four reference boranes cover an FIA range from 287.7 kJ/mol for Mes_3B to 331.8 kJ/mol for BPh_3 and 471.4 kJ/mol for $B(C_6F_5)_3$. From Mes_3B to BPh_3 Lewis-acidity increases because the Mes-groups are successively replaced by the less sterically shielding and less electron rich phenyl-rings. Still, BPh_3 is rated as only moderately Lewis-acidic, while $B(C_6F_5)_3$ is a benchmark for strong Lewis acids.
The FIA of the synthesized boranes cover a range from 302.5 J/mol (**4a**) to 359.5 kJ/mol (**4d**). Borane **4i**, which could not be accessed via the described route, gave a lower FIA of 294.1 kJ/mol.
To put these results into perspective, while **4a**-**4h** can be regarded as more sterically crowded than Mes_2BPh, they all exhibit FIAs equal (**4a**) or higher than this reference compound. The FIAs of the acceptor substituted **4d** (359.5 kJ/mol) and the bifunctional **4g** (345.1 kJ/mol) even exceed the FIA of BPh_3. While even **4d** and **4g** must still be regarded as only moderately Lewis-acidic, these results indicate that the chemical transformation reported herein allows to incrementally vary the Lewis acidity of a given borane precursor over a very broad range, even in the presence of other highly sterically shielding substituents on boron.

Conclusion

In summary, we have reported the conversion of a tetrazolyl-functionalized borane precursor into a series of eight boranes bearing oxadiazolyl-groups with chemically and electronically diverse substituents. The molecular structure allows for intra-molecular N→B-coordination and provides full conjugation between the boron-center and the peripheral substituents.
A full characterization of the optical, electrochemical and electronic properties, both experimentally and by DFT calculations showed that the borane exhibit dynamic N→B-coordination with ***open*** and ***closed*** conformers of most borane existing in dynamic equilibrium. ^{11}B NMR indicates that only systems with the strongest acceptor (**4h**, 5-CF_3-functionalized oxadiazole) exclusively adopt the ***open*** conformation.
Our most intriguing find is that the fluorescence behavior in particular varies drastically among the individual compounds in the presence of strong nucleophiles (F^-, CN^-). While differing degrees of fluorescence quenching is observed in most cases, **4c** (4-OMe-Phenyl) and **4g** (bifunctional) exhibit fluorescence shift (4g) and selective enhancement upon bind of CN^-.
These results show that the synthetic strategy would offer a versatile synthetic access to libraries of tailored dyes, fluorescent sensors and Lewis acids.

Supporting Information

The supporting information contains descriptions of materials and instruments used, detailed synthetic procedures, and addition analytical data not depicted in the main article. The latter includes NMR (^1H, ^{13}C, ^{11}B), optical spectra, electrochemical data, mass spectrometry data, and details on crystallographic data collection, and computational results including optimized computed structures, orbital- and spin-density-plots, and tddft-results. Comprehensive supporting information has been uploaded to https://zenodo.org and can be accessed under DOI: 10.5281/zenodo.17866757.

Crystallographic data for has also been uploaded at the Cambridge Crystallographic Data Center (CCDC, https://www.ccdc.cam.ac.uk/) under deposition numbers CCDC-2514222 through CCDC-2514226 for compounds **4a**, **4b**, **4c**, **4f** and **8b**.

The authors have cited additional references within the Supporting Information.[95–102]

Acknowledgements

JS and FP thank the German Science Foundation (DFG, German Research Foundation, project number FP 2217/4-1) and the German Chemical Industry Fund (FCI, Liebig scholarship to FP) for financial support. Prof. Orthaber thanks the Swedish Research Council (Vetenskapsrådet) for support.

Keywords: boranes • oxadiazoles • turn-on fluorescence • anion sensors • Lewis acids

References

1 W. Zhang and Y. Jin, *Dynamic Covalent Chemistry: Principles, Reactions, and Applications*, John Wiley & Sons, Hoboken, 2017.
2 M. Barboiu, Ed., *Constitutional Dynamic Chemistry*, Springer Berlin

View Article Online
DOI: 10.1039/D5OB01979F

Heidelberg, Berlin, Heidelberg, 2012, vol. 322.

3 A. J. M. Miller, Controlling ligand binding for tunable and switchable catalysis: cation-modulated hemilability in pincer-crown ether ligands, *Dalton Trans.*, 2017, **46**, 11987–12000.

4 S. E. Angell, C. W. Rogers, Y. Zhang, M. O. Wolf and W. E. Jones, Hemilabile coordination complexes for sensing applications, *Coord. Chem. Rev.*, 2006, **250**, 1829–1841.

5 T. Baumgartner and F. Jäkle, *Main Group Strategies towards Functional Hybrid Materials*, John Wiley & Sons, 2008.

6 A. Doshi and F. Jäkle, in *Comprehensive Inorganic Chemistry II*, Elsevier, 2013, pp. 861–891.

7 Y. Ren and F. Jäkle, Merging thiophene with boron: new building blocks for conjugated materials, *Dalton Trans.*, 2016, **45**, 13996–14007.

8 F. Jäkle, in *Synthesis and Application of Organoboron Compounds. Topics in Organometallic Chemistry, vol 49.*, eds. E. Fernández and A. Whiting, Springer, Cham, 2015, pp. 297–325.

9 F. Jäkle, Lewis acidic organoboron polymers, *Coord. Chem. Rev.*, 2006, **250**, 1107–1121.

10 F. Jäkle, Advances in the Synthesis of Organoborane Polymers for Optical, Electronic, and Sensory Applications, *Chem. Rev.*, 2010, **110**, 3985–4022.

11 F. Jäkle, in *Encyclopedia of Inorganic Chemistry*, ed. R. B. King, Wiley & Sons Ltd, 2005.

12 C. D. Entwistle and T. B. Marder, Applications of Three-Coordinate Organoboron Compounds and Polymers in Optoelectronics, *Chem. Mater.*, 2004, **16**, 4574–4585.

13 C. D. Entwistle and T. B. Marder, Die Borchemie leuchtet: optische Eigenschaften von MolekÃ¼len und Polymeren, *Angew. Chem.*, 2002, **114**, 3051.

14 D. Shimoyama and F. Jäkle, Controlling the aggregation and assembly of boron-containing molecular and polymeric materials, *Aggregate*, DOI:10.1002/agt2.149.

15 E. A. Patrick and W. E. Piers, Twenty-five years of bis-pentafluorophenyl borane: a versatile reagent for catalyst and materials synthesis, *Chem. Commun.*, 2020, **56**, 841–853.

16 E. von Grotthuss, A. John, T. Kaese and M. Wagner, Doping Polycyclic Aromatics with Boron for Superior Performance in Materials Science and Catalysis, *Asian J. Org. Chem.*, 2018, **7**, 37–53.

17 L. Ji, S. Griesbeck and T. B. Marder, Recent developments in and perspectives on three-coordinate boron materials: a bright future, *Chem. Sci.*, 2017, **8**, 846–863.

18 X. Long, J. Yao, F. Cheng, C. Dou and Y. Xia, Double B←N bridged bipyridine-containing polymer acceptors with enhanced electron mobility for all-polymer solar cells, *Mater. Chem. Front.*, 2019, **3**, 70–77.

19 X. Long, Z. Ding, C. Dou, J. Liu and L. Wang, A double B←N bridged bipyridine (BNBP)-based polymer electron acceptor: all-polymer solar cells with a high donor : acceptor blend ratio, *Mater. Chem. Front.*, 2017, **1**, 852–858.

20 R. Zhao, C. Dou, Z. Xie, J. Liu and L. Wang, Polymer Acceptor Based on B←N Units with Enhanced Electron Mobility for Efficient All-Polymer Solar Cells, *Angew. Chem. Int. Ed.*, 2016, **55**, 5313–5317.

21 X. Long, Y. Gao, H. Tian, C. Dou, D. Yan, Y. Geng, J. Liu and L. Wang, Electron-transporting polymers based on a double B←N bridged bipyridine (BNBP) unit, *Chem. Commun.*, 2017, **53**, 1649–1652.

22 X. Long, Z. Ding, C. Dou, J. Zhang, J. Liu and L. Wang, Polymer Acceptor Based on Double B←N Bridged Bipyridine (BNBP) Unit for High-Efficiency All-Polymer Solar Cells, *Adv. Mater.*, 2016, **28**, 6504–6508.

23 C. Dou, J. Liu and L. Wang, Conjugated polymers containing B←N unit as electron acceptors for all-polymer solar cells, *Sci. China Chem.*, 2017, **60**, 450–459.

24 M. Grandl, J. Schepper, S. Maity, A. Peukert, E. Von Hauff and F. Pammer, N → B Ladder Polymers Prepared by Postfunctionalization: Tuning of Electron Affinity and Evaluation as Acceptors in All-Polymer Solar Cells, *Macromolecules*, 2019, **52**, 1013–1024.

25 M. Vanga, A. Sahoo, R. A. Lalancette and F. Jäkle, Linear Extension of Anthracene via B←N Lewis Pair Formation: Effects on Optoelectronic Properties and Singlet O 2 Sensitization, *Angew. Chem.*, 2022, **134**, e202113075.

26 A. Wakamiya, T. Taniguchi and S. Yamaguchi, Intramolecular B–N Coordination as a Scaffold for Electron-Transporting Materials: Synthesis and Properties of Boryl-Substituted Thienylthiazoles, *Angew. Chem.*, 2006, **118**, 3242–3245.

27 D.-T. Yang, J. Radtke, S. K. Mellerup, K. Yuan, X. Wang, M. Wagner and S. Wang, One-Pot Synthesis of Brightly Fluorescent Mes2B-Functionalized Indolizine Derivatives via Cycloaddition Reactions, *Org. Lett.*, 2015, **17**, 2486–2489.

28 D. R. Levine, M. A. Siegler and J. D. Tovar, Thiophene-Fused Borepins As Directly Functionalizable Boron-Containing π-Electron Systems, *J. Am. Chem. Soc.*, 2014, **136**, 7132–7139.

29 C. Reus, S. Weidlich, M. Bolte, H.-W. Lerner and M. Wagner, C-Functionalized, Air- and Water-Stable 9,10-Dihydro-9,10-diboraanthracenes: Efficient Blue to Red Emitting Luminophores, *J. Am. Chem. Soc.*, 2013, **135**, 12892–12907.

30 A. Wakamiya, K. Mori and S. Yamaguchi, 3-Boryl-2,2′-bithiophene as a Versatile Core Skeleton for Full-Color Highly Emissive Organic Solids, *Angew. Chem. Int. Ed.*, 2007, **46**, 4273–4276.

31 F. Vidal, J. McQuade, R. Lalancette and F. Jäkle, ROMP-Boranes as Moisture-Tolerant and Recyclable Lewis Acid Organocatalysts, *J. Am. Chem. Soc.*, 2020, **142**, 14427–14431.

32 H. Lin, S. Patel and F. Jäkle, Tailored Triarylborane Polymers as Supported Catalysts and Luminescent Materials, *Macromolecules*, 2020, **53**, 10601–10612.

33 T. Kushida and S. Yamaguchi, A Radical Anion of Structurally Constrained Triphenylborane, *Organometallics*, 2013, **32**, 6654–6657.

34 X. Yin, J. Chen, R. A. Lalancette, T. B. Marder and F. Jäkle, Highly Electron-Deficient and Air-Stable Conjugated Thienylboranes, *Angew. Chem.*, 2014, **126**, 9919–9923.

35 X. Yin, F. Guo, R. A. Lalancette and F. Jäkle, Luminescent Main-Chain Organoborane Polymers: Highly Robust, Electron-Deficient Poly(oligothiophene borane)s via Stille Coupling Polymerization, *Macromolecules*, 2016, **49**, 537–546.

36 V. M. Hertz, N. Ando, M. Hirai, M. Bolte, H.-W. Lerner, S. Yamaguchi and M. Wagner, Steric Shielding vs Structural Constraint in a Boron-Containing Polycyclic Aromatic Hydrocarbon, *Organometallics*, 2017, **36**, 2512–2519.

37 N. Baser-Kirazli, R. A. Lalancette and F. Jäkle, Tuning the

View Article Online
DOI: 10.1039/D5OB01979F

Donor−π–Acceptor Character of Arylborane–Arylamine Macrocycles, *Organometallics*, 2021, **40**, 520–528.

38 Z. Yang, K. Yang, X. Wei, W. Liu, R. Gao, F. Jäkle, Y.-L. Loo and Y. Ren, A Multiple Excited-State Engineering of Boron-Functionalized Diazapentacene Via a Tuning of the Molecular Orbital Coupling, *J. Phys. Chem. Lett.*, 2021, **12**, 9308–9314.

39 P. Li, D. Shimoyama, N. Zhang, Y. Jia, G. Hu, C. Li, X. Yin, N. Wang, F. Jäkle and P. Chen, A New Platform of B/N-Doped Cyclophanes: Access to a π-Conjugated Block-Type B 3 N 3 Macrocycle with Strong Dipole Moment and Unique Optoelectronic Properties, *Angew. Chem. Int. Ed.*, 2022, **61**, e202200612.

40 A. F. Alahmadi, X. Yin, R. A. Lalancette and F. Jäkle, Synthesis and Structure-Property Relationships in Regioisomeric Alternating Borane-Terthiophene Polymers, *Chem. Eur. J.*, DOI:10.1002/chem.202203619.

41 I. B. Sivaev and V. I. Bregadze, Lewis acidity of boron compounds, *Coord. Chem. Rev.*, 2014, **270**–**271**, 75–88.

42 R. J. Mayer, N. Hampel and A. R. Ofial, Lewis Acidic Boranes , Lewis Bases , and Equilibrium Constants : A Reliable Scaffold for a Quantitative Lewis Acidity / Basicity Scale, *Angew. Chem. Int. Ed.*, 2008, **47**, 7659–7663.

43 L. O. Müller, D. Himmel, J. Stauffer, G. Steinfeld, J. Slattery, G. Santiso-Quinones, V. Brecht and I. Krossing, Angew Chem Int Ed - 2008 - Müller - Simple Access to the Non-Oxidizing Lewis Superacid PhF->Al(ORF)3 RF= C(CF3)3, *Angew. Chem. Int. Ed.*, 2008, **47**, 7659–7663.

44 M. Fontani, F. Peters, W. Scherer, W. Wachter, M. Wagner and P. Zanello, Adducts of Ferrocenylboranes and Pyridine Bases: Generation of Charge-Transfer Complexes and Reversible Coordination Polymers, *Eur. J. Inorg. Chem.*, 1998, **1998**, 1453–1465.

45 A. F. Alahmadi, J. Zuo and F. Jäkle, B-N Lewis pair-fused dipyridylfluorene copolymers incorporating electron-deficient benzothiadiazole comonomers, *Polym. J.*, 2023, **55**, 433–442.

46 J. Zuo, K. Liu, J. Harrell, L. Fang, P. Piotrowiak, D. Shimoyama, R. A. Lalancette and F. Jäkle, Near-IR Emissive B–N Lewis Pair-Functionalized Anthracenes via Selective LUMO Extension in Conjugated Dimer and Polymer, *Angew. Chem. Int. Ed.*, 2024, **63**, e202411855.

47 M. Vanga, A. Sahoo, R. A. Lalancette and F. Jäkle, Linear Extension of Anthracene via B←N Lewis Pair Formation: Effects on Optoelectronic Properties and Singlet O 2 Sensitization, *Angew. Chem. Int. Ed.*, 2022, **61**, e202113075.

48 Y. Shi, Y. Zeng, P. Kucheryavy, X. Yin, K. Zhang, G. Meng, J. Chen, Q. Zhu, N. Wang, X. Zheng, F. Jäkle and P. Chen, Dynamic B/N Lewis Pairs: Insights into the Structural Variations and Photochromism via Light-Induced Fluorescence to Phosphorescence Switching, *Angew. Chem. Int. Ed.*, 2022, **61**, e202213615.

49 R. P. Nandi, J. Zuo and F. Jaekle, B-N Fused Anthracene as Functional Linker for π-Extended Viologens: Near-IR Emission and Electrochromism, *Angew. Chem.*, 2026, **138**, e21634.

50 J. Miao, Y. Wang, J. Liu and L. Wang, Organoboron molecules and polymers for organic solar cell applications, *Chem. Soc. Rev.*, 2022, **51**, 153–187.

51 S. Wang, D. Yang, J. Lu, H. Shimogawa, S. Gong, X. Wang, S. K. Mellerup, A. Wakamiya, Y. Chang, C. Yang and Z. Lu, In Situ Solid-State Generation of (BN)2-Pyrenes and Electroluminescent Devices, *Angew. Chem. Int. Ed.*, 2015, **54**, 15074–15078.

52 R. Hecht, J. Kade, D. Schmidt and A. Nowak-Król, n-Channel Organic Semiconductors Derived from Air-Stable Four-Coordinate Boron Complexes of Substituted Thienylthiazoles, *Chem. Eur. J.*, 2017, **23**, 11620–11628.

53 M. Liu, D. Zhou, Y. B. He, Y. Fu, X. Qin, C. Miao, H. Du, B. Li, Q. H. Yang, Z. Lin, T. S. Zhao and F. Kang, Novel gel polymer electrolyte for high-performance lithium-sulfur batteries, *Nano Energy*, 2016, **22**, 278–289.

54 X. Zhang, F. Rauch, J. Niedens, R. B. da Silva, A. Friedrich, A. Nowak-Król, S. J. Garden and T. B. Marder, Electrophilic C–H Borylation of Aza[5]helicenes Leading to Bowl-Shaped Quasi-[7]Circulenes with Switchable Dynamics, *J. Am. Chem. Soc.*, 2022, **144**, 22316–22324.

55 D. Volland, J. Niedens, P. T. Geppert, M. J. Wildervanck, F. Full and A. Nowak-Król, Synthesis of a Blue-Emissive Azaborathia[9]helicene by Silicon-Boron Exchange from Unusual Atropisomeric Teraryls, *Angew. Chem. Int. Ed.*, DOI:10.1002/anie.202304291.

56 F. Full, Q. Wölflick, K. Radacki, H. Braunschweig and A. Nowak-Król, Enhanced Optical Properties of Azaborole Helicenes by Lateral and Helical Extension, *Chem. Eur. J.*, DOI:10.1002/chem.202202280.

57 R. Koch, Y. Sun, A. Orthaber, A. J. Pierik and F. Pammer, Turn-on fluorescence sensors based on dynamic intramolecular N→B-coordination, *Org. Chem. Front.*, 2020, **7**, 1437–1452.

58 S. Schraff, Y. Sun and F. Pammer, Tuning of electronic properties via labile N→B-coordination in conjugated organoboranes, *J. Mater. Chem. C*, 2017, **5**, 1730–1741.

59 J. Schepper, A. Orthaber and F. Pammer, Tetrazole-Functionalized Organoboranes Exhibiting Dynamic Intramolecular N→B-Coordination and Cyanide-Selective Anion Binding, *Chem. – A Eur. J.*, 2024, **30**, e202401466.

60 J. Chen, R. A. Lalancette and F. Jäkle, Chiral Organoborane Lewis Pairs Derived from Pyridylferrocene, *Chem. Eur. J.*, 2014, **20**, 9120–9129.

61 S. Schwendemann, R. Fröhlich, G. Kehr and G. Erker, Intramolecular frustrated N/B lewis pairs by enamine hydroboration, *Chem. Sci.*, 2011, **2**, 1842.

62 G.-Q. Chen, F. Türkyilmaz, C. G. Daniliuc, C. Bannwarth, S. Grimme, G. Kehr and G. Erker, Enamine/butadienylborane cycloaddition in the frustrated Lewis pair regime, *Org. Biomol. Chem.*, 2015, **13**, 10477–10486.

63 C. Zeng, K. Yuan, N. Wang, T. Peng, G. Wu and S. Wang, The opposite and amplifying effect of B ← N coordination on photophysical properties of regioisomers with an unsymmetrical backbone, *Chem. Sci.*, 2019, **10**, 1724–1734.

64 Y. Cao, J. K. Nagle, M. O. Wolf and B. O. Patrick, Tunable Luminescence of Bithiophene-Based Flexible Lewis Pairs, *J. Am. Chem. Soc.*, 2015, **137**, 4888–4891.

65 Y. Cao, N. E. Arsenault, D. Hean and M. O. Wolf, Fluorescence Switching of Intramolecular Lewis Acid–Base Pairs on a Flexible Backbone, *J. Org. Chem.*, 2019, **84**, 5394–5403.

66 C. T. Hoang, I. Prokes, G. J. Clarkson, M. J. Rowland, J. H. R. Tucker, M. Shipman and T. R. Walsh, Study of boron–nitrogen dative bonds using azetidine inversion dynamics, *Chem. Commun.*,

View Article Online
DOI: 10.1039/D5OB01979F

2013, **49**, 2509.

67 S. J. Cassidy, I. Brettell-Adams, L. E. McNamara, M. F. Smith, M. Bautista, H. Cao, M. Vasiliu, D. L. Gerlach, F. Qu, N. I. Hammer, D. A. Dixon and P. A. Rupar, Boranes with Ultra-High Stokes Shift Fluorescence, *Organometallics*, 2018, **37**, 3732–3741.

68 Y. Shi, J. Wang, H. Li, G. Hu, X. Li, S. K. Mellerup, N. Wang, T. Peng and S. Wang, A simple multi-responsive system based on aldehyde functionalized amino-boranes, *Chem. Sci.*, 2018, **9**, 1902–1911.

69 Z. M. Hudson and S. Wang, Impact of Donor−Acceptor Geometry and Metal Chelation on Photophysical Properties and Applications of Triarylboranes, *Acc. Chem. Res.*, 2009, **42**, 1584–1596.

70 C. R. Wade, A. E. J. J. Broomsgrove, S. Aldridge and F. P. Gabbaï, Fluoride ion complexation and sensing using organoboron compounds, *Chem. Rev.*, 2010, **110**, 3958–3984.

71 N. Ishida, T. Moriya, T. Goya and M. Murakami, Synthesis of Pyridine−Borane Complexes via Electrophilic Aromatic Borylation, *J. Org. Chem.*, 2010, **75**, 8709–8712.

72 S. A. Iqbal, J. Pahl, K. Yuan and M. J. Ingleson, Intramolecular (directed) electrophilic C–H borylation, *Chem. Soc. Rev.*, 2020, **49**, 4564–4591.

73 M. Grandl, B. Rudolf, Y. Sun, D. F. Bechtel, A. J. Pierik and F. Pammer, Intramolecular N→B Coordination as a Stabilizing Scaffold for π-Conjugated Radical Anions with Tunable Redox Potentials, *Organometallics*, 2017, **36**, 2527–2535.

74 M. Grandl, Y. Sun and F. Pammer, Generation of an N→B Ladder-type Structure by Regioselective Hydroboration of an Alkenyl-Functionalized Quaterpyridine, *Chem. Eur. J.*, 2016, **22**, 3976–3980.

75 M. Grandl, T. Kaese, A. Krautsieder, Y. Sun and F. Pammer, Hydroboration as an Efficient Tool for the Preparation of Electronically and Structurally Diverse N→B-Heterocycles, *Chem. Eur. J.*, 2016, **22**, 14373–14382.

76 M. Grandl, Y. Sun and F. Pammer, Electronic and structural properties of N → B-ladder boranes with high electron affinity, *Org. Chem. Front.*, 2018, **5**, 336–352.

77 F. Pammer, J. Schepper, J. Glöckler, Y. Sun and A. Orthaber, Expansion of the scope of alkylboryl-bridged N → B-ladder boranes: New substituents and alternative substrates, *Dalton Trans.*, 2019, **48**, 10298–10312.

78 M. Grandl and F. Pammer, Preparation of Head-to-Tail Regioregular 6-(1-Alkenyl)-Functionalized Poly(pyridine-2,5-diyl) and its Post-Functionalization via Hydroboration, *Macromol. Chem. Phys.*, 2015, **216**, 2249–2262.

79 K. Yuan, N. Suzuki, S. K. Mellerup, X. Wang, S. Yamaguchi and S. Wang, Pyridyl Directed Catalyst-Free trans -Hydroboration of Internal Alkynes, *Org. Lett.*, 2016, **18**, 720–723.

80 J. D. W. Schepper, A. Orthaber and F. Pammer, Preparation of Structurally and Electronically Diverse N → B-Ladder Boranes by [2 + 2 + 2] Cycloaddition, *J. Org. Chem.*, 2021, **86**, 14767–14776.

81 B. Reichart and C. O. Kappe, High-temperature continuous flow synthesis of 1,3,4-oxadiazoles via N-acylation of 5-substituted tetrazoles, *Tetrahedron Lett.*, 2012, **53**, 952–955.

82 R. Huisgen, J. Sauer and H. J. Sturm, Acylierung 5-substituierter Tetrazole zu 1.3.4-Oxdiazolen, *Angew. Chem.*, 1958, **9**, 272–273.

83 V. K. Gour, S. Yahya and M. Shahar Yar, Unveiling the chemistry of 1,3,4-oxadiazoles and thiadiazols: A comprehensive review, *Arch. Pharm.*, 2024, **357**, 2300328.

84 J. Lu, I. Persson, H. Lind, J. Palisaitis, M. Li, Y. Li, K. Chen, J. Zhou, S. Du, Z. Chai, Z. Huang, L. Hultman, P. Eklund, J. Rosen, Q. Huang and P. O. Å. Persson, Tin+1Cn MXenes with fully saturated and thermally stable Cl terminations, *Nanoscale Adv.*, 2019, **1**, 3680–3685.

85 U. Mitschke and P. Bäuerle, The electroluminescence of organic materials, *J. Mater. Chem.*, 2000, **10**, 1471–1507.

86 R. Deng, L. Li, M. Song, S. Zhao, L. Zhou and S. Yao, Synthesis and optoelectronic properties of oxadiazole coordinated boron complexes, *CrystEngComm.*, 2016, **18**, 4382–4387.

87 D. Zhou, D. Liu, X. Gong, H. Ma, G. Qian, S. Gong, G. Xie, W. Zhu and Y. Wang, Solution-Processed Highly Efficient Bluish-Green Thermally Activated Delayed Fluorescence Emitter Bearing an Asymmetric Oxadiazole–Difluoroboron Double Acceptor, *ACS Appl. Mater. Interfaces*, 2019, **11**, 24339–24348.

88 L. I. Vereshchagin, O. N. Verkhozina, F. A. Pokatilov and V. N. Kizhnyaev, Synthesis of 2-Substituted 5-Trifluoromethyl-1 , 3 , 4-oxadiazoles, *Russ. J. Org. Chem.*, 2007, **43**, 1575–1576.

89 C. Hansch, A. Leo and R. W. Taft, A Survey of Hammett Substituent Constants and Resonance and Field Parameters, *Chem. Rev.*, 1991, **91**, 165–195.

90 N. M. D. Brown, F. Davidson and J. W. Wilson, Dimesitylboryl compounds, *J. Organomet. Chem.*, 1981, **209**, 1–11.

91 C. D. Good and D. M. Ritter, Alkenylboranes. II. Improved Preparative Methods and New Observations on Methylvinylboranes, *J. Am. Chem. Soc.*, 1962, **84**, 1162–1166.

92 N. Hoshi, K. Sasaki, S. Hashimoto and Y. Hori, Electrochemical dechlorination of chlorobenzene with a mediator on various metal electrodes, *J. Electroanal. Chem.*, 2004, **568**, 267–271.

93 H. Jung, R. H. Heflich, P. P. Fu, A. U. Shaikh and P. E. Hartman, Nitro group orientation, reduction potential, and direct-acting mutagenicity of nitro-polycyclic aromatic hydrocarbons, *Environ. Mol. Mutagen.*, 1991, **17**, 169–180.

94 C. M. Cardona, W. Li, A. E. Kaifer, D. Stockdale and G. C. Bazan, Electrochemical Considerations for Determining Absolute Frontier Orbital Energy Levels of Conjugated Polymers for Solar Cell Applications, *Adv. Mater.*, 2011, **23**, 2367–2371.

95 W. L. . Armarego and D. D. Perrin, *Purification of laboratory chemicals*, Butterworth-Heinemann, Oxford, 4th edn., 1997.

96 G. R. Fulmer, A. J. M. Miller, N. H. Sherden, H. E. Gottlieb, A. Nudelman, B. M. Stoltz, J. E. Bercaw and K. I. Goldberg, NMR Chemical Shifts of Trace Impurities: Common Laboratory Solvents, Organics, and Gases in Deuterated Solvents Relevant to the Organometallic Chemist, *Organometallics*, 2010, **29**, 2176–2179.

97 S. Ando and T. Matsuura, Substituent shielding parameters of fluorine-19 NMR on polyfluoroaromatic compounds dissolved in dimethyl sulphoxide- d 6, *Magn. Reson. Chem.*, 1995, **33**, 639–645.

98 P. Mani, A. K. Singh and S. K. Awasthi, AgNO3catalyzed synthesis of 5-substituted-1H-tetrazole via [3+2] cycloaddition of nitriles and sodium azide Dedicated to the memory of late Dr. Tarkeshwar Gupta, *Tetrahedron Lett.*, 2014, **55**, 1879–1882.

99 I. V. Bliznets, A. A. Vasil'ev, S. V. Shorshnev, A. E. Stepanov and S. M. Lukyanov, Microwave-assisted synthesis of sterically hindered 3-(5-tetrazolyl) pyridines, *Tetrahedron Lett.*, 2004, **45**, 2571–2573.

100 B. Akhlaghinia and S. Rezazadeh, A Novel Approach for the Synthesis of 5-Substituted-1, *J. Brazilian Chem. Soc.*, 2012, **23**, 2197–2203.

View Article Online
DOI: 10.1039/D5OB01979F

101 B. Du, X. Jiang and P. Sun, Palladium-Catalyzed Highly Selective ortho -Halogenation (I, Br, Cl) of Arylnitriles via sp 2 C–H Bond Activation Using Cyano as Directing Group, *J. Org. Chem.*, 2013, **78**, 2786–2791.

102 G. M. Sheldrick, A short history of SHELX, *Acta Crystallogr. Sect. A Found. Crystallogr.*, 2008, **64**, 112–122.

Taylor & Francis Group
an informa business

View Article Online
DOI: 10.1039/D5OB01979F

Data availability statement

All analytical data associated with the publication will be made available online through an online repository.

Details see below

Availability of data	Template data availability statement
Data openly available in a public repository that issues datasets with DOIs	The data that support the findings of this book/chapter are openly available in https://zenodo.org/ at https://zenodo.org/records/17866758

Ulm, 09 December 2025, PD Dr, Frank Pammer